ELSEVIER

Global minima of protonated water clusters

Matthew P. Hodges [a,*], David J. Wales [b]

[a] *School of Chemistry, University of Nottingham, University Park, Nottingham, NG7 2RD, UK*
[b] *University Chemical Laboratory, University of Cambridge, Lensfield Road, Cambridge, CB2 1EW, UK*

Abstract

Candidate global minima are obtained for $H_3O^+ \cdots (H_2O)_n$ clusters with $n \leqslant 20$ using a basin-hopping algorithm and an empirical, polarizable model potential. We have reoptimized the lowest minima for each system using a more accurate model and find extensive reordering of the potential energy surfaces, especially for larger n. For both model potentials a distorted dodecahedron surrounding an H_2O molecule is the global minimum for $n = 20$, in good agreement with experiment. The gap between the latter structure and the lowest minimum with H_3O^+ in the centre is about 10–20 kJ mol^{-1}. © 2000 Elsevier Science B.V. All rights reserved.

1. Introduction

There have been many previous studies of protonated water clusters at various levels of theory. The most accurate calculations have, of course, been conducted for the smallest systems; overviews of the literature for $n = 1$ and $n = 2$ can be found in our recent studies of rearrangement mechanisms in these clusters [1,2]. Benchmark calculations on $H_5O_2^+$ by Valeev and Schaefer are noteworthy for revealing the sensitivity of the potential energy surface (PES) to basis set and correlation effects [3]. Other studies have employed a variety of techniques including MP2, density functional theory (DFT) and semi-empirical methods [4–10].

For larger systems, model potentials parametrized using experimental or ab initio data provide a com-

putationally efficient alternative to more accurate techniques. One early study by David [11] used a polarization model [12] to optimize a dodecahedral structure for $n = 20$. Kozack and Jordan developed empirical interaction potentials for $H^+ \cdots H_2O$ and $H_3O^+ \cdots H_2O$, which we refer to as KJ(H$^+$) and KJ(H$_3$O$^+$) respectively, and used them to study $n \leqslant 6$ [13] and later $n = 19$–21 clusters [14]. Corongui et al. [15] complemented DFT calculations with results based on a model potential composed of the MCY form [16] for the $H_2O \cdots H_2O$ interactions and a potential developed by Fornili et al. [17] for the $H_3O^+ \cdots H_2O$ interactions. One of us has developed a sophisticated anisotropic site potential (ASP) [18] and used this to study the structure and energetics of clusters with $n = 1$–7, and more recently Shevkunov and Vegiri [19] developed another potential and applied it to clusters up to about $n = 50$. The KJ(H$^+$) potential has also been used by Svanberg and Pettersson [20] in Monte Carlo simulations

* Corresponding author. Fax: +44-115-951-3562; e-mail: pczmph@unix.ccc.nottingham.ac.uk

for $n = 8$, 20 and 39. These are just a few examples of previous theoretical studies, and a useful review of the subject has been presented by Kochanski et al. which includes a historical account of the study of these systems, discussing the use of the various methods mentioned above [21].

The most basic structural question one can ask is the geometry of the global potential energy minimum of the cluster. If it is kinetically accessible on the experimental timescale then this minimum will dominate the low temperature behaviour of the system. The problem of global minimization has been studied quite extensively for atomic systems and proteins (for a recent overview see Ref. [22]) and we recently published a study for neutral water clusters containing up to 21 molecules [23] using the empirical TIP4P potential [24], supplemented with more accurate energy evaluations using the polarizable ASP-W4 model [25]. In Ref. [23] putative global minima were located using the basin-hopping technique [26] and the conclusions of our study have since found support in further calculations by Day et al. [27]. Here we present an analogous study for the case of protonated water clusters. The only previous basin-hopping study that we know of for any of these systems was performed by Singer et al. [28] who used it to complement jump-walking Monte Carlo (MC) simulations. The MC calculations were not successful in locating the global minimum for $n = 7$ and numerous lower-energy minima were found using the basin-hopping technique. For $n = 15$, only MC calculations were performed, and a minimum was constructed by hand that was lower in energy than those previously found, even though this structure was approximately planar with considerably fewer hydrogen bonds than would be expected for 3-dimensional morphologies.

Our aim in this contribution is to search the PESs of protonated water clusters to locate low-energy minima and to identify favourable morphologies. The coordinates of our lowest energy structures will be made available for downloading from the Cambridge Cluster Database [29]. One concern with some of the previous studies is that rather limited sets of configurations have been considered, and we intend to generate a large database of minima that will be made available as a reference for more accurate calculations. To illustrate the scale of the problem of searching the potential energy surfaces for these clusters, we note the work of McDonald et al. [30] who used graph theoretical techniques to enumerate the number of viable minima for cubic morphologies with $n = 7$ and dodecahedral morphologies with $n = 19$. This method provides a systematic way of investigating the possible hydrogen-bonding patterns for a given set of locations of the oxygen atoms. For $n = 7$, 11 initial configurations were generated from which six minima were obtained using a model potential from the OSS family [31]. For $n = 19$, the number of hydrogen-bonding topologies was found to be nearly 90 000 for structures including a H_3O^+ unit acting as triple proton donor, of which about 200 were selected for further analysis using an empirically determined fitness criterion based on topological properties. The above study illustrates that a comprehensive sampling of low-energy structures is likely to become computationally unfeasible even for quite small clusters, and that locating the global minimum for the larger systems will be a very challenging problem. As we noted for neutral water clusters [23], the interplay of centre-of-mass and angular degrees of freedom produces a more complex PES than for atomic clusters with a similar number of degrees of freedom.

2. Methods

The details of the global optimization calculations are much the same as in our previous study [23], though here we use the $KJ(H_3O^+)$ model potential of Kozack and Jordan [13]. All calculations were performed with a modified version of the Orient program [32]. We performed preliminary runs of 30 000 quenches for $n = 9$ starting from randomly generated geometries, with various temperatures and acceptance ratios, and a common lowest-energy minimum was found in all runs. The minimum number of quenches needed to find it for any one run was 70, and the maximum was 3360. The most successful set of parameters combined a temperature of 0.4 kJ mol^{-1} and an acceptance ratio of 0.4. For this combination the global minimum was found on average after 291 quenches. The final centre-of-mass and

angular steps were about 2.2 bohr and 0.83 radians and we used these as starting values in all the subsequent runs.

The $KJ(H_3O^+)$ potential uses both rigid H_3O^+ and H_2O molecules and comprises point charges on all the H_3O^+ and H_2O atoms, with one additional charge on the C_2 axis for H_2O. For both molecules

isotropic dipole–dipole polarizabilities are included and we calculate the induction energy to first order. The dispersion-repulsion model is a simple Lennard-Jones 6-12 form with interactions centred on the H_3O^+ oxygen atom and the fourth charge site of the H_2O molecule. We found that neglecting the induction term led to qualitative changes in the

Table 1
Energies (kJ mol^{-1}) of the lowest three minima found for the $KJ(H_3O^+)$ potential in each basin-hopping run for $H_3O^+ \cdots (H_2O)_n$ and the number of the quench at which the minimum was first found

n	Energy 1	Quench 1	Energy 2	Quench 2	Energy 3	Quench 3
1	− 116.47	1				
2	− 220.95	1	− 173.15	34	− 172.27	1228
3	− 314.97	1	− 281.53	5	− 274.27	50
4	− 372.12	7	− 364.09	57	− 360.85	7913
5	− 424.13	404	− 423.56	332	− 422.06	2493
6	− 480.11	179	− 479.29	189	− 478.20	116
7	− 530.67	68	− 530.46	74	− 530.11	62
8	− 587.52	29	− 586.42	213	− 584.34	37
9	− 638.39	932	− 637.73	950	− 637.38	964
10	− 690.56	4716	− 689.03	5192	− 688.59	279
	− 690.56	386	− 690.55	1353	− 689.03	1480
	− 690.56	78	− 690.55	8148	− 689.03	141
11	− 742.67	421	− 742.50	1068	− 741.86	1876
	− 742.67	6651	− 742.50	671	− 741.86	1384
	− 742.67	5225	− 742.50	3712	− 741.86	3049
12	− 791.08	93	− 790.90	193	− 789.61	2744
	− 794.44	4606	− 790.78	4828	− 789.61	4643
	− 794.44	7503	− 790.78	6683	− 789.86	1698
13	− 840.89	4031	− 839.29	3986	− 839.04	4543
	− 843.80	1745	− 842.42	1283	− 842.04	1255
	− 843.80	8718	− 842.42	8673	− 842.04	8672
14	− 890.57	314	− 889.00	640	− 888.81	12046
	− 890.57	8956	− 889.00	5821	− 888.81	6823
	− 893.51	9929	− 893.05	10003	− 892.29	11787
15	− 943.19	8197	− 942.50	8641	− 942.36	8348
	− 941.35	1051	− 940.41	1044	− 938.85	19393
	− 940.55	190	− 939.78	224	− 938.81	252
16	− 997.17	15663	− 996.63	16603	− 995.89	15771
	− 997.17	28242	− 996.63	1435	− 995.89	28316
	− 993.51	14435	− 993.34	7176	− 992.66	7154
17	− 1039.79	696	− 1039.54	18944	− 1038.87	13438
	− 1040.72	439	− 1040.10	17627	− 1039.21	1260
	− 1033.75	10461	− 1032.84	11475	− 1031.98	10633
18	− 1096.36	6570	− 1095.58	26951	− 1095.26	6497
	− 1096.36	14561	− 1096.11	14698	− 1095.52	1208
	− 1096.69	18944	− 1096.36	4316	− 1096.11	4405
19	− 1143.98	10689	− 1143.20	10124	− 1143.03	23932
	− 1143.94	6108	− 1143.75	4361	− 1143.20	4355
	− 1134.57	1298	− 1134.28	3084	− 1132.17	8539
20	− 1183.85	5311	− 1183.60	5090	− 1182.29	4334
	− 1202.92	11676	− 1202.60	2323	− 1201.76	4225
	− 1194.60	24077	− 1192.97	14193	− 1192.68	3827

potential energy surfaces for small clusters and rejected this simplified version of the $KJ(H_3O^+)$ model, even though using a polarizable model reduced the number of quenches that we were able to perform for each run. For the TIP4P model in our previous basin-hopping calculations it was computationally feasible to perform 100 000 quenches even for $(H_2O)_{20}$.

We have reoptimized up to fifty of the lowest-energy minima found for each $KJ(H_3O^+)$ basin-hopping run using a more accurate anisotropic site potential (ASP) model [18]. This ASP model comprises accurate long-range electrostatics with distributed multipoles up to hexadecapole on all atoms, polariz-

abilities up to quadrupole–quadrupole terms on the oxygen atoms, anisotropic repulsion and charge-transfer terms fitted using intermolecular perturbation theory (IMPT) calculations [33] and a damped atom–atom dispersion model. The implications of using rigid-monomer models have been discussed before [18] where calculations using the ASP models for the $H_3O^+ \cdots H_2O$ and $H_2O \cdots H_2O$ interactions were compared with DFT results. It was found that even though the ASP model is not able to quantitatively describe the shared proton in $H_5O_2^+$ units in clusters, the geometry of $H_5O_2^+$ is reproduced reasonably well in terms of the oxygen–oxygen separation and the location of the free hydro-

Table 2

Energies (kJ mol^{-1}) of the lowest 10 minima found in basin-hopping runs for $H_3O^+ \cdots (H_2O)_n$ with the $KJ(H_3O^+)$ potential

1	2	3	4	5	6	7
− 116.47	− 220.95	− 314.97	− 372.12	− 424.13	− 480.11	− 530.67
	− 173.15	− 281.53	− 364.09	− 423.56	− 479.29	− 530.46
	− 172.27	− 274.27	− 360.85	− 422.06	− 478.20	− 530.11
		− 273.39	− 333.55	− 421.41	− 477.40	− 529.96
		− 223.85	− 331.24	− 419.85	− 475.84	− 529.21
		− 213.09	− 328.68	− 419.22	− 475.45	− 529.15
			− 328.60	− 419.13	− 475.12	− 528.34
			− 325.35	− 418.78	− 474.94	− 528.20
			− 321.81	− 417.69	− 474.71	− 528.09
				− 417.43	− 473.92	− 527.96

8	9	10	11	12	13	14
− 587.52	− 638.39	− 690.56	− 742.67	− 794.44	− 843.80	− 893.51
− 586.42	− 637.73	− 690.55	− 742.50	− 791.08	− 842.42	− 893.05
− 584.34	− 637.38	− 689.03	− 741.86	− 790.90	− 842.04	− 892.29
− 583.45	− 636.87	− 688.59	− 741.63	− 790.78	− 841.98	− 890.69
− 583.09	− 635.90	− 688.55	− 740.83	− 789.86	− 841.48	− 890.57
− 582.05	− 635.76	− 688.50	− 740.40	− 789.61	− 840.89	− 890.30
− 581.88	− 635.31	− 688.42	− 739.80	− 789.51	− 840.52	− 890.20
− 581.49	− 634.74	− 688.20	− 739.38	− 788.55	− 839.29	− 889.47
− 581.09	− 634.61	− 687.75	− 739.30	− 788.27	− 839.24	− 889.00
− 580.80	− 634.45	− 687.60	− 739.15	− 788.16	− 839.12	− 888.97

15	16	17	18	19	20
− 943.19	− 997.17	− 1040.72	− 1096.69	− 1143.98	− 1202.92
− 942.50	− 996.63	− 1040.10	− 1096.36	− 1143.94	− 1202.60
− 942.36	− 995.89	− 1039.79	− 1096.11	− 1143.75	− 1201.76
− 941.35	− 994.09	− 1039.54	− 1095.58	− 1143.20	− 1201.39
− 940.55	− 993.51	− 1039.21	− 1095.52	− 1143.03	− 1200.58
− 940.41	− 993.49	− 1038.87	− 1095.33	− 1142.60	− 1199.67
− 940.20	− 993.34	− 1038.64	− 1095.26	− 1142.38	− 1199.53
− 940.11	− 993.05	− 1038.56	− 1095.15	− 1142.07	− 1199.33
− 939.78	− 993.01	− 1038.24	− 1095.13	− 1141.99	− 1199.30
− 939.02	− 992.66	− 1037.98	− 1094.97	− 1141.82	− 1198.19

gen atoms. A cyclic minimum for $H_3O^+ \cdots (H_2O)_4$ was also located similar to a structure found in an

earlier study [15] based on an $H_5O_2^+$ unit plus three H_2O molecules.

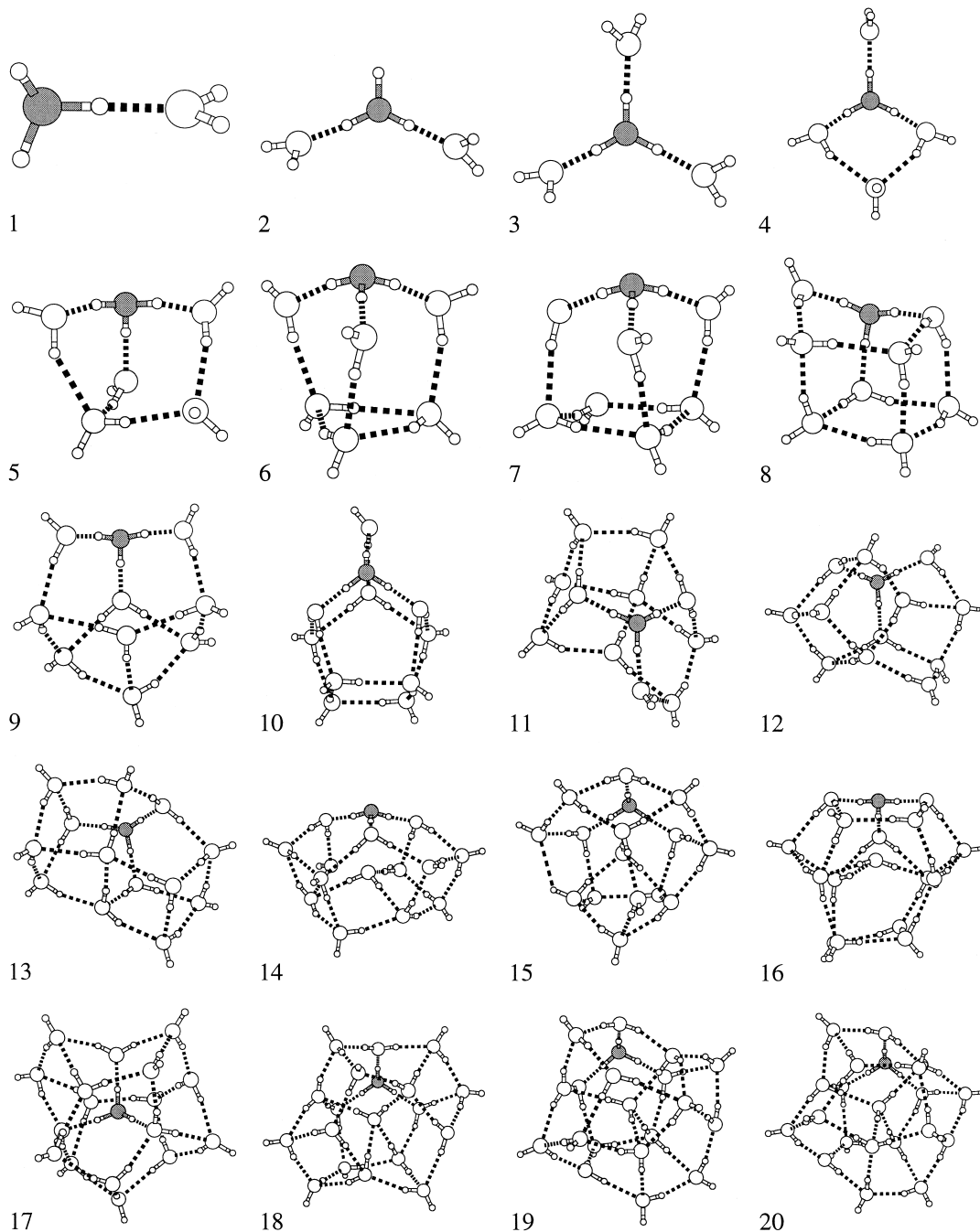Fig. 1. Putative global minima found using the KJ(H_3O^+) potential for $H_3O^+ \cdots (H_2O)_n$ with $1 \leqslant n \leqslant 20$. The oxygen on each H_3O^+ ion is shaded to distinguish it.

3. Results

3.1. Basin-hopping with the KJ(H₃O⁺) model

3.1. Basin-hopping with the $KJ(H_3O^+)$ model

One or three basin-hopping runs, consisting of 30 000 quenches each, were performed for $n \leqslant 9$ and $n = 10–20$, respectively. The lowest three energies found and the quench at which they were first located are collected in Table 1. The lowest 10 energies are given in Table 2. For $n < 10$, the lowest-energy minimum was located in under 1000 quenches in all cases and there is little doubt these are the global minima for this particular potential. For $n = 10–20$ the likelihood that we have found the true global minimum decreases with n, but we can be reasonably confident that we have found the global minimum when the same structure is found in all three of the independent runs. This is the case for $n = 10$ and 11, while for $n = 12$, 13 and 16 the same lowest-energy minimum was found in two of the three runs. For $n = 14$ and 15 we performed one additional run, but in both cases we neither found a new putative global minimum nor the one previously located. The candidate global minima for $n \geqslant 17$ may well be bettered in the future.

Our lowest minima for $n = 1–20$ are shown in Fig. 1. For $n = 1–3$ they are chain-like, including a branched chain for $n = 3$. For $n \geqslant 4$, the structures are dominated by 4-membered and 5-membered rings and only for $n = 4$ do we find a water molecule outside a closed ring. Dodecahedral fragments are evident in many of the clusters, for example, it can be clearly seen that for $n = 9$ and $n = 15$ the H_3O^+ molecule is a member of two and three pentagonal rings, respectively. For $n \geqslant 15$, the global minima are all clathrate structures with a central H_2O molecule, except for $n = 17$, which has a central H_3O^+ ion. For $n = 20$, the lowest minimum found is a distorted dodecahedron. This result is in agreement with previous studies, though we believe that this is the first time that a dodecahedron has been located from a random starting geometry. For $n = 19$ and 20, we find no evidence of low-energy minima based on the fused cube and edge-sharing pentagonal prism morphologies which have recently been studied by Khan [34].

The relative stabilities of each pair of clusters with n and $(n - 1)$ H_2O molecules are shown in Fig. 2. For $n \geqslant 4$ the stabilities of adjacent clusters are reasonably consistent, all of them falling between
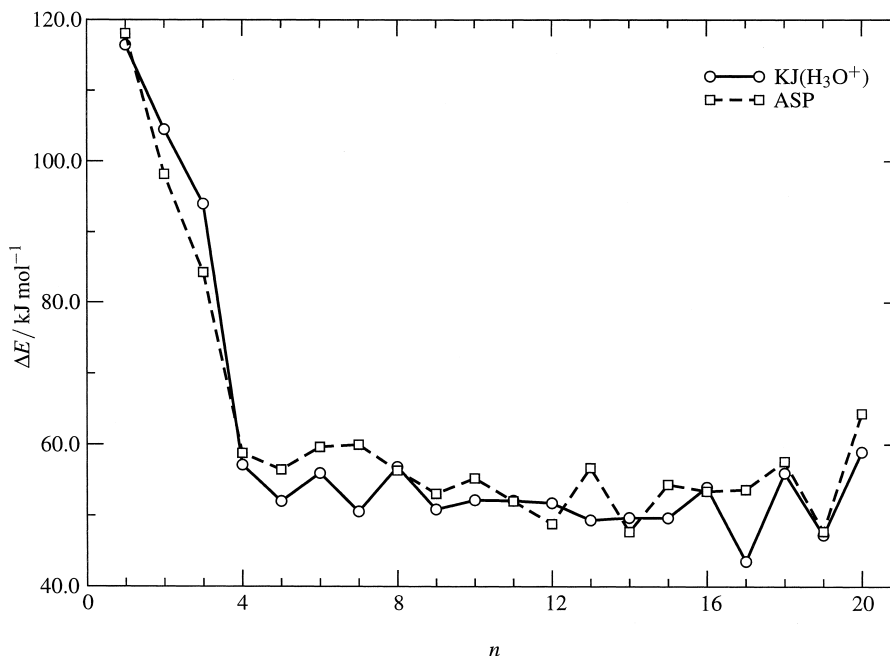

Fig. 2. Energy differences (ΔE) between global minima for the process $H_3O^+ \cdots (H_2O)_n \rightarrow H_3O^+ \cdots (H_2O)_{n-1} + H_2O$.

40 and 60 kJ mol^{-1}. Above $n = 3$, where the first solvation shell is completed, the dodecahedron at $n = 20$ is the most stable with respect to loss of a water molecule. This result is interesting in the light of experiments where $n = 20$ is found to be a 'magic number' under a range of experimental conditions [35]. Furthermore, it has been shown that for mixed clusters with trimethylamine (TMA) the optimum number of TMA molecules coordinated to H_3O^+ $\cdots (H_2O)_{20}$ is 10. This number is consistent with a dodecahedral structure with the H_3O^+ molecule in the centre, where the 10 hydrogens not involved in hydrogen bonds in the outer cage are free to associate with the TMA ligands. However, in our lowest minimum for $n = 20$ the H_3O^+ is in the cage and only nine hydrogens on the surface are not involved in hydrogen bonding.

To further investigate the dodecahedral minima we performed a number of additional basin-hopping runs of 10 000 quenches only taking steps in the angular degrees of freedom. This procedure enables us to sample different hydrogen-bonding arrangements for a given set of centre-of-mass coordinates. The first set of centre-of-mass coordinates was taken from the lowest-energy minimum found for $n = 20$, namely the distorted dodecahedron. The second was constructed by taking the distorted dodecahedron and exchanging the positions of the central H_2O and H_3O^+ molecules. The third and fourth sets of coordinates were constructed by taking the lowest-energy regular dodecahedron found in our neutral water study and adding respectively a H_2O and H_3O^+ molecule at the centre of the cage. We refer to these four morphologies as distorted/H_2O, distorted/

H_3O^+, regular/H_2O and regular/H_3O^+ respectively, and the lowest 10 energies found from each of the four runs are given in Table 3. None of the runs resulted in a minimum lower in energy than had already been found from the conventional basin-hopping runs. Reoptimizing the structures found in the regular/H_2O and regular/H_3O^+ runs always resulted in distortion of the dodecahedron facilitating the formation of hydrogen bonds between the central molecule and those in the shell around it. The lowest minimum, at -1202.92 kJ mol^{-1}, is stabilized by four hydrogen bonds to the central H_2O molecule, such that the two donor protons point towards the centre of the cluster, approximately towards the acceptor lone pairs. The lowest H_3O^+-centered cluster is about 10 kJ mol^{-1} less strongly bound at -1192.72 kJ mol^{-1}. In this case, the H_3O^+ molecule acts as a hydrogen-bond donor to three water molecules, leaving 10 hydrogen atoms not involved in hydrogen bonds, which is consistent with the TMA experiments [35]. We note, however, that the difference in energies for the H_3O^+-centered and H_2O-centered structures is small, and that the KJ(H_3O^+) potential may not be accurate enough to predict the energetic ordering of these different morphologies correctly. Also, finite temperature effects may be important when comparing theoretical and experimental results, since entropy will alter the relative stabilities of different structures [36]. Ligation by TMA could also affect the relative stabilities, of course.

An indication of the number of minima close in energy to the candidate global minimum can be found in Table 2. For $n \leqslant 4$ there is a significant gap

Table 3
Energies (kJ mol^{-1}) of the lowest 10 minima found in basin-hopping runs with the KJ(H_3O^+) potential employing only angular steps for four dodecahedral morphogies of H_3O^+ $\cdots (H_2O)_{20}$

Distorted/H_2O	Distorted/H_3O^+	Regular/H_2O	Regular/H_3O^+
-1202.92	-1188.19	-1191.27	-1192.72
-1201.76	-1182.58	-1174.89	-1190.84
-1201.39	-1179.60	-1174.14	-1190.33
-1200.58	-1178.90	-1171.62	-1189.89
-1200.57	-1177.76	-1170.32	-1185.54
-1199.33	-1176.68	-1170.31	-1183.09
-1199.28	-1176.35	-1169.74	-1182.75
-1198.17	-1175.85	-1169.31	-1178.95
-1197.63	-1175.49	-1169.04	-1178.18
-1196.03	-1174.69	-1167.42	-1177.43

between the global minimum and the next lowest, but for larger clusters many minima can be very close in energy. For example, at $n = 18$ the lowest 10 minima found lie within a range of about 1.7 kJ mol^{-1}, some of which represent different hydrogen-bonding patterns for similar centre-of-mass coordinates. All 10 of these have 31 hydrogen bonds suggesting that the hydrogen-bonding network is of great importance in the ordering of low-energy structures.

3.2. Reoptimizations with the ASP potential

We now describe reoptimizations of the minima found from the KJ(H$_3$O$^+$) basin-hopping runs using the more sophisticated ASP model. First we compare with the lowest-energy minima found in the original ASP study (Ref. [18]) in which minima for $n \leqslant 7$ were located using MC simulations. For both $n = 5$ and 6, the basin-hopping runs have bettered the lowest-energy minima previously found by about 0.27 and and 0.35 kJ mol^{-1} respectively. For $n = 5$, the structural differences are principally in the orientations of the hydrogen atoms on the H$_2$O molecules bonded to H$_3$O$^+$, but for $n = 6$, the differences are more significant and the new lowest-energy minimum is similar to that found with the KJ(H$_3$O$^+$) model as shown in Fig. 1. The relative energies for the loss of one H$_2$O molecule are shown in Fig. 2

Table 4
Energies (kJ mol^{-1}) of the lowest 10 minima found in basin-hopping runs for H$_3$O$^+ \cdots$ (H$_2$O)$_n$ after reoptimisation with the ASP potential

1		2		3		4		5		6		7	
− 118.07	1	− 216.27	1	− 300.52	1	− 359.31	1	− 415.77	13	− 475.42	1	− 535.39	22
		− 214.56	2	− 298.33	5	− 357.84	4	− 415.50	15	− 475.07	6	− 535.16	6
				− 281.95	2	− 355.59	4	− 415.48	1	− 474.98	5	− 533.09	1
				− 279.07	6	− 353.25	2	− 414.77	14	− 474.06	2	− 531.78	3
				− 274.79	4	− 336.65	6	− 414.26	2	− 473.54	16	− 530.96	34
						− 335.36	5	− 411.51	3	− 472.89	20	− 530.08	13
								− 411.13	10	− 472.59	4	− 530.05	17
								− 410.89	9	− 472.59	4	− 529.95	12
								− 410.87		− 472.30	13	− 529.13	25
								− 410.61	4	− 472.16	7	− 529.04	27

8		9		10		11		12		13		14	
− 591.73	2	− 644.81	3	− 700.05	3	− 752.07	2	− 800.91	4	− 857.63	1	− 905.36	93
− 590.18	1	− 643.94	1	− 699.02	6	− 750.62	55	− 799.98	38	− 856.86	4	− 904.94	55
− 589.45	3	− 642.74	2	− 698.50	8	− 749.99	36	− 799.69	1	− 856.81	48	− 901.81	50
− 588.72		− 642.43	4	− 697.08	10	− 749.86	5	− 799.39	39	− 856.53	51	− 900.66	1
− 586.51	8	− 641.79	19	− 696.21	33	− 749.84	3	− 799.08	8	− 856.16	27	− 900.65	45
− 586.30	15	− 641.52	13	− 695.65	32	− 749.66	58	− 798.98	108	− 855.81	77	− 899.35	51
− 586.13	21	− 641.14	10	− 695.17	7	− 747.11	23	− 798.29	81	− 854.45	59	− 899.30	62
− 585.82	30	− 641.13	27	− 694.15	9	− 747.09	33	− 798.25	10	− 854.01	6	− 899.20	4
− 585.75		− 641.02	9	− 693.93	15	− 746.91	16	− 798.19	43	− 854.00	5	− 896.63	13
− 585.26	19	− 639.69	29	− 693.83	13	− 746.60	63	− 797.87	21	− 853.45	44	− 895.86	20

15		16		17		18		19		20	
− 959.71	6	− 1013.12	24	− 1066.76	75	− 1124.38	19	− 1172.18	10	− 1236.52	8
− 959.56	4	− 1011.77	64	− 1064.12	62	− 1122.35	67	− 1171.07	29	− 1235.68	1
− 958.27	131	− 1010.08	95	− 1063.19	96	− 1122.27	11	− 1170.98	48	− 1235.51	3
− 957.38	60	− 1009.74	121	− 1060.55	102	− 1121.64	96	− 1170.89	72	− 1235.32	2
− 957.18	45	− 1008.46	6	− 1054.71		− 1121.03	20	− 1170.77	1	− 1235.07	6
− 956.74	89	− 1008.43	9	− 1054.62	85	− 1120.92	1	− 1170.60	6	− 1234.78	4
− 956.09		− 1008.28	34	− 1054.32	34	− 1120.65	15	− 1169.99	39	− 1234.69	7
− 955.98	57	− 1008.15	19	− 1054.10	118	− 1120.56	2	− 1169.76	51	− 1232.19	48
− 955.88	20	− 1007.91	30	− 1053.56	67	− 1120.45	14	− 1169.56	9	− 1231.63	5
− 955.01	71	− 1006.82	3	− 1052.94	111	− 1120.25	26	− 1169.19	28	− 1230.93	13

along with the KJ(H_3O^+) results that were discussed in Section 3.1. The general trends are similar to the KJ(H_3O^+) results: for $n = 1$–3, the values are high because a strong hydrogen bond to H_3O^+ has to be broken; for $n \geqslant 4$, the majority of the dissociation energies are between 50 and 60 kJ mol^{-1}; the loss of H_2O at $n = 20$ is again the most unfavourable for $n > 3$ and the energy difference between the $n = 19$ and 20 lowest-energy structures is about 64.3 kJ mol^{-1}, compared with 58.9 kJ mol^{-1} for KJ(H_3O^+).

The energies of the lowest 10 ASP minima are given for each n in Table 4 along with the index of the corresponding KJ(H_3O^+) minimum, ranked according to energy, from which it was relaxed (the absence of this second number indicates that the ASP minimum was optimized from a KJ(H_3O^+) minimum that was not formally converged). For $n = 1$–4, 6 and 13 the lowest ASP minimum was obtained from the lowest KJ(H_3O^+) minimum, and these pairs of minima are qualitatively very similar, with only minor differences in the orientations of the hydrogen atoms not involved in hydrogen bonding. For $n = 1$ the ASP minimum better represents the C_2 structure found from ab initio calculations than the KJ(H_3O^+) minimum, as was previously reported [18]. For $n = 5$, the framework of oxygen atoms is similar, but the lowest-energy ASP minimum has eight hydrogen bonds rather than the seven found with KJ(H_3O^+). In this case, the ASP minimum was obtained from the 13th lowest KJ(H_3O^+) minimum, which is book-like with two fused 4-membered rings, and the energy difference between the minima with seven and eight hydrogen bonds is about 0.3 kJ mol^{-1}. For $n = 7$ the lowest ASP minimum is cube-like with 12 hydrogen bonds, whereas the KJ(H_3O^+) minimum contains 4-membered and 5-membered rings and has 10 hydrogen bonds. In this case, the lowest ASP minimum was obtained from the 22nd lowest KJ(H_3O^+) minimum, which has 11 hydrogen bonds, and the cube is formed when a 6-membered ring closes to form two 4-membered rings in its place. This cube-like structure is similar to the global minimum for $(H_2O)_8$, but in general we find that the morphologies of the $H_3O^+ \cdots (H_2O)_n$ and $(H_2O)_{n+1}$ global minima are quite different. For $n = 8$ and $n = 10$, the lowest ASP and KJ(H_3O^+) minima are similar whereas for $n = 9$ they differ substantially, although both have 14 hy-

drogen bonds. For larger n it is clear from Table 4 that the ordering of the minima on the two potential energies surfaces can vary quite significantly. For example, for $n = 14$ the lowest ASP minimum was obtained from the KJ(H_3O^+) minimum ranked 93rd in energy, although the difference in energy between this structure and the putative global minimum using the KJ(H_3O^+) potential is only about 12 kJ mol^{-1}.

Clathrate structures with a central H_2O molecule are found for $n = 16$, and 18–20. For the KJ(H_3O^+) potential there is also a central H_3O^+ ion for $n = 17$. For $n = 20$ the dodecahedron is again the dominant morphology. In fact the energetic ordering of the KJ(H_3O^+) and ASP minima is much more consistent here than for any of the other larger clusters to the extent that the lowest eight KJ(H_3O^+) structures are found amongst the lowest 10 ASP minima. We have also reoptimized the minima obtained from the angle-only basin-hopping runs and find the lowest H_2O-centered and H_3O^+-centered structures at -1236.52 (located in the original reoptimizations) and -1214.26 kJ mol^{-1} respectively. This energy difference is somewhat larger than found with the KJ(H_3O^+) potential.

4. Conclusions

We have performed basin-hopping simulations with the empirical KJ(H_3O^+) model potential for a number of protonated water clusters and have presented candidate global minima up to $n = 20$. There does not usually appear to be any connection between the $H_3O^+ \cdots (H_2O)_n$ and $(H_2O)_{n+1}$ global minima. The protonated water clusters are generally more disordered than their neutral counterparts and it is likely that the additional proton has a large influence on the local structure. Clathrate structures are found as the lowest-energy minima for $n \geqslant 15$, and for $n = 20$ the global minimum is a distorted dodecahedron with a central H_2O molecule. Experimental results suggest that structures containing a central H_3O^+ ion are dominant and the lowest such minimum lies about 10 kJ mol^{-1} above the global minimum in the present work.

Calculations with a more sophisticated ASP model reveal many qualitative as well as quantitative differences in the potential energy surfaces, though gen-

eral trends in the energetics of the clusters are similar. In particular, both potentials find the $n = 20$ cluster to be the most stable with respect to loss of one water molecule for $n > 3$. This enhanced stability is greater for the ASP model, and these results indicate that energetic factors may contribute to the experimental observation of $n = 20$ as a magic number.

Acknowledgements

References

[1] D.J. Wales, J. Chem. Phys. 110 (1999) 10403.
[2] D.J. Wales, J. Chem. Phys. 111 (1999) 8429.
[3] E.F. Valeev, H.F. Schaefer, J. Chem. Phys. 108 (1998) 7197.
[4] E.P.F. Lee, J.M. Dyke, Mol. Phys. 73 (1991) 375.
[5] D.Q. Wei, D.R. Salahub, J. Chem. Phys. 101 (1994) 7633.
[6] A. Khan, Chem. Phys. Lett. 217 (1994) 443.
[7] K. Laasonen, M.L. Klein, J. Phys. Chem. 98 (1994) 10079.
[8] D.Q. Wei, D.R. Salahub, J. Chem. Phys. 106 (1997) 6086.
[9] Y.V. Novakovskaya, N.F. Stepanov, J. Phys. Chem. A 103 (1999) 3285.
[10] J.-C. Jiang, Y.-S. Wang, H.-C. Chang, S.H. Lin, Y.T. Lee, G. Niedner-Schatteburg, H.-C. Chang, J. Am. Chem. Soc. 122 (2000) 1398.
[11] C.W. David, J. Mol. Struct. (THEOCHEM) 150 (1987) 391.
[12] F.H. Stillinger, C.W. David, J. Chem. Phys. 69 (1978) 1473.
[13] R.E. Kozack, P.C. Jordan, J. Chem. Phys. 96 (1992) 3131.
[14] R.E. Kozack, P.C. Jordan, J. Chem. Phys. 99 (1993) 2978.
[15] G. Corongiu, R. Kelterbaum, E. Kochanski, J. Phys. Chem. 99 (1995) 8038.
[16] O. Matsuoka, E. Clementi, M. Yoshimine, J. Chem. Phys. 64 (1976) 1351.
[17] S.L. Fornili, M. Migliore, M.A. Palazzo, Chem. Phys. Lett. 125 (1986) 419.
[18] M.P. Hodges, A.J. Stone, J. Chem. Phys. 110 (1999) 6766.
[19] S.V. Shevkunov, A. Vegiri, J. Chem. Phys. 111 (1999) 9303.
[20] M. Svanberg, J.B.C. Pettersson, J. Phys. Chem. A 102 (1998) 1865.
[21] E. Kochanski, R. Kelterbaum, S. Klein, M.M. Rohmer, A. Rahmouni, Adv. Quantum Chem. 28 (1997) 273.
[22] D.J. Wales, H.A. Scheraga, Science 285 (1999) 1368.
[23] D.J. Wales, M.P. Hodges, Chem. Phys. Lett. 286 (1998) 65.
[24] W.L. Jorgensen, J. Chandrasekhar, J.D. Madura, R.W. Impey, M.L. Klein, J. Chem. Phys. 79 (1983) 926.
[25] C. Millot, J.C. Soetens, M.T.C.M. Costa, M.P. Hodges, A.J. Stone, J. Phys. Chem. A 102 (1998) 754.
[26] Z. Li, H.A. Scheraga, Proc. Natl. Acad. Sci. USA 84 (1987) 6611.
[27] P.N. Day, R. Pachter, M.S. Gordon, G.N. Merrill, J. Chem. Phys. 112 (2000) 2063.
[28] S.J. Singer, S. McDonald, L. Ojamäe, J. Chem. Phys. 112 (2000) 710.
[29] D.J. Wales, J.P.K. Doye, A. Dullweber, F.Y. Naumkin, M.P. Hodges, 2000, The Cambridge Cluster Database, URL http://brian.ch.cam.ac.uk.
[30] S. McDonald, L. Ojamäe, S.J. Singer, J. Phys. Chem. A 102 (1998) 2824.
[31] L. Ojamäe, I. Shavitt, S.J. Singer, J. Chem. Phys. 109 (1998) 5547.
[32] A.J. Stone, A. Dullweber, M.P. Hodges, P.L.A. Popelier, D.J. Wales, Orient, University of Cambridge, 3rd edn., 1997.
[33] I.C. Hayes, A.J. Stone, Mol. Phys. 53 (1984) 83.
[34] A. Khan, Chem. Phys. Lett. 319 (2000) 440.
[35] S. Wei, Z. Shi, A.W. Castleman, J. Chem. Phys. 94 (1991) 3268.
[36] Z. Shi, J.V. Ford, S. Wei, A.W. Castleman, J. Chem. Phys. 99 (1993) 8009.